Onset and Progression of Peripapillary Retinal Nerve Fiber Layer (RNFL) Retardance Changes Occur Earlier Than RNFL Thickness Changes in Experimental Glaucoma

Brad Fortune, Claude F. Burgoyne, Grant Cull, Juan Reynaud, and Lin Wang

Discoveries in Sight Research Laboratories, Devers Eye Institute and Legacy Research Institute, Legacy Health, Portland, Oregon

Correspondence: Brad Fortune, Associate Scientist, Devers Eye Institute, 1225 NE Second Avenue, Portland, OR 97232; bfortune@deverseye.org.

Submitted: April 12, 2013
Accepted: June 11, 2013

Citation: Fortune B, Burgoyne CF, Cull G, Reynaud J, Wang L. Onset and progression of peripapillary retinal nerve fiber layer (RNFL) retardance changes occur earlier than RNFL thickness changes in experimental glaucoma. *Invest Ophthalmol Vis Sci*. 2013;54:5653–5660. DOI:10.1167/iovs.13-12219

Purpose. Longitudinal measurements of peripapillary RNFL thickness and retardance were compared in terms of time to reach onset of damage and time to reach a specific progression endpoint.

Methods. A total of 41 rhesus macaques with unilateral experimental glaucoma (EG) each had three or more weekly baseline measurements in both eyes of peripapillary RNFL thickness (RNFLT) and retardance. Laser photocoagulation was then applied to the trabecular meshwork of one eye to induce chronic elevation of intraocular pressure and weekly imaging continued. Pairwise differences between baseline observations were sampled by bootstrapping to determine the 95% confidence limits of each measurement's repeatability. The first two sequential measurements below the lower confidence limit defined the endpoint for each parameter. Segmented linear and exponential decay functions were fit to each RNFL-versus-time series to determine the time to damage onset.

Results. In all, 29 (71%) of the EG eyes reached endpoint by RNFL retardance and 25 (61%) reached endpoint by RNFLT. In total, 33 (80%) reached endpoint by at least one of the RNFL parameters and 21 (51%) reached endpoint by both RNFL parameters. Of the 33 EG eyes reaching any endpoint, a larger proportion reached endpoint first by retardance ($n = 26$, 79%) than did by RNFLT ($n = 7$, 21%; $P = 0.002$). Survival analysis indicated a shorter time to reach endpoint by retardance than by RNFLT ($P < 0.001$). Of the 21 EG eyes that reached endpoint by both measures, the median duration to endpoint was 120 days for retardance and 223 days for RNFLT ($P = 0.003$, Wilcoxon test). The time to onset was faster for retardance than that for RNFLT based on either segmented fits (by 31 days; $P = 0.008$, average $R^2 = 0.89$) or exponential fits (by 102 days; $P = 0.01$, average $R^2 = 0.89$).

Conclusions. The onset of progressive loss of RNFL retardance occurs earlier than the onset of RNFL thinning. Endpoints of progressive loss from baseline also occurred more frequently and earlier for RNFL retardance as compared with RNFLT.

Keywords: glaucoma, retinal ganglion cell, retinal nerve fiber layer, scanning laser polarimetry, birefringence, optical coherence tomography

The peripapillary retinal nerve fiber layer (RNFL) is an important structural feature to examine and monitor for diagnosis and management of glaucoma patients.[1–3] RNFL thickness can be measured accurately and reliably by optical coherence tomography (OCT),[4,5] although recent evidence from experimental glaucoma in nonhuman primates indicates that peripapillary RNFL thickness does not begin to decline until 10%–15% of axons are already lost from the anterior orbital (retrobulbar) optic nerve[6] and not until after substantial deformation of the optic nerve head (ONH) surface and subsurface structures has already occurred.[7,8] Thus, it is possible that mechanisms of glaucomatous injury have already begun to damage axons prior to the point that loss of RNFL thickness can be detected by OCT. Scanning laser polarimetry (SLP) is an alternative mode of imaging designed to measure the relative phase retardance induced by birefringent tissues such as the RNFL.[9] It is thought that the normal RNFL exhibits strong birefringence due to the highly ordered structural array of cytoskeletal proteins within its axons.[10–14] Recent evidence demonstrates that RNFL retardance measured by polarimetry declines prior to loss of RNFL thickness measured by OCT in experimental models of retinal ganglion cell (RGC) axonal injury including experimental glaucoma.[8,13,15]

In our previous study comparing peripapillary RNFL retardance with thickness,[8] we focused on a specific time point representing a relatively early stage of experimental glaucoma. Specifically, we performed the comparison of RNFL parameters around the onset of ONH surface topography change measured by confocal scanning laser tomography. We found that at this early time point, RNFL retardance had already begun to decline, whereas RNFL thickness did not exhibit any change until after onset of ONH surface topography change, at which point loss of RNFL retardance had progressed even further.[8] RGC-specific functional loss was also present prior to the onset of ONH surface topography change or loss of RNFL thickness and these functional changes had also progressed by the time RNFL thickness had begun to decline.[8] We concluded that the findings were consistent with a pathologic sequence

whereby axonal cytoskeletal disruption precedes thinning and total degeneration of axons within the RNFL.

In the current study, we further test this hypothesis by evaluating the entire longitudinal series of RNFL retardance and thickness independently of ONH surface topography. We perform a "trend analysis" to compare the time to reach onset of progressive loss by RNFL retardance versus thickness and an "event analysis" to compare the time to reach an endpoint by each RNFL parameter. The null hypothesis is that no difference between RNFL parameters should exist for either the duration to reach onset or the duration to reach endpoint. The results demonstrate unequivocally that both the onset and endpoint of progressive loss are reached earlier by RNFL retardance and that endpoints are reached first much more frequently by RNFL retardance than by RNFL thickness.

Methods

Subjects

The subjects of this study were 41 rhesus macaque monkeys (*Macaca mulatta*). Table 1 lists the age, weight, and sex of each animal. A small fraction of the RNFL data from 33 of these 41 animals was presented previously.[8] All experimental methods and animal care procedures adhered to the Association for Research in Vision and Ophthalmology's Statement for the Use of Animals in Ophthalmic and Vision Research and were approved and monitored by the Institutional Animal Care and Use Committee at Legacy Health.

Anesthesia

All experimental procedures began with induction of general anesthesia using ketamine (15 mg/kg, administered intramuscularly [IM]) in combination with either xylazine (0.8–1.5 mg/kg IM) or midazolam (0.2 mg/kg, IM), along with a single subcutaneous injection of atropine sulfate (0.05 mg/kg). Animals were then intubated and breathed isoflurane gas (1%–2%; typically 1.25%) mixed with oxygen to maintain anesthesia during all imaging procedures. A clear, rigid gas-permeable contact lens filled with 0.5% carboxymethylcellulose solution was placed over the apex of each cornea. Heart rate and arterial oxyhemoglobin saturation were monitored continuously and maintained above 75/min and 95%, respectively. Body temperature was maintained at 37°C.

Peripapillary RNFL Thickness

Peripapillary RNFL thickness was measured using spectral-domain OCT (SD-OCT, Spectralis; Heidelberg Engineering GmbH, Heidelberg, Germany) as previously described.[8] For this study, the average peripapillary RNFL thickness was measured from a single circular B-scan consisting of 1536 A-scans. Nine to 16 individual sweeps were averaged in real time to comprise the final stored B-scan at each session. The position of the scan was centered on the ONH at the first imaging session and all follow-up scans were pinned (identical) to this location. A trained technician masked to the purpose of this study manually corrected the accuracy of the instrument's native automated layer segmentations when the algorithm had obviously erred from the inner and outer borders of the RNFL to an adjacent layer (such as a refractive element in the vitreous instead of the internal limiting membrane, or to the outer border of the inner plexiform layer instead of the RNFL). All SD-OCT scans in this study (1677 in total) had an acceptable quality score above 15 (98% were >20; 56% were >30, median score was 31).

Peripapillary RNFL Retardance

Peripapillary RNFL retardance measurements were obtained by SLP using a commercial glaucoma workup device (GDxVCC instrument; Carl Zeiss Meditec, Inc., Dublin, CA) as previously described.[8,13,15,16] The instrument compensates for the effects of anterior segment (primarily corneal) birefringence to more accurately determine RNFL birefringence.[17,18] A bite bar, which rotates in three axes, was used to properly align the head and eye, and autorefraction was used for each scan. Three RNFL scans were averaged for each eye at each time point. The GDxVCC instrument detects the relative phase retardance of a cross-polarized source after a double pass through the tissue sample, assumes that RNFL thickness is linearly related to retardance, then calculates and reports an estimate of RNFL "thickness" using a linear conversion factor of 1.67 μm/nm[9] (as stated in the instrument manual[19]). Values of RNFL "thickness" were exported for the "small" peripapillary locus, which is an 8-pixel-wide band centered on the optic disc, with a mean scan radius of 4.84 degrees,[19] corresponding to approximately 1.12 mm on the macaque retina.[15] The average of the 64 exported peripapillary samples was taken as the summary parameter for each eye and time point.

Intraocular Pressure (IOP) Measurements

IOP was measured in both eyes at the start of every session using an applanation tonometer (Tonopen XL; Reichert Technologies, Inc., Depew, NY). The value recorded for each eye was the average of three successive measurements.

Experimental Design and Protocol

Each animal had a minimum of three (average of five) weekly baseline recordings for each of the above-described peripapillary RNFL measurements. Argon laser photocoagulation was then applied to the trabecular meshwork of one eye of each animal to induce chronic elevation of IOP.[20,21] Initially, 180° of the trabecular meshwork was treated in one session, after which the remaining 180° was treated in a second session approximately 2 weeks later. If necessary, laser treatments were repeated in subsequent weeks (limited to a 90° sector) until an IOP elevation was first noted or if the initial postlaser IOP had returned to normal levels. The average number of laser treatments (±SD) was 5.6 ± 2.9.

Weekly measurements continued during the postlaser follow-up period in alternating fashion such that SD-OCT scans to measure RNFL thickness were acquired 1 week, then SLP scans to measure RNFL retardance were acquired the following week; thus, each measurement of a given type was separated by approximately 2 weeks. This schedule continued for each animal until its predefined sacrifice target had been reached. Specific targets for the EG stage when each animal was sacrificed were based on the primary study to which each animal was assigned and were predetermined based on those protocols. Thus the EG stage at sacrifice and details of sacrifice procedures differed across animals.

Analysis and Statistics

An "event analysis" was used to compare the time (from first laser) to reach an endpoint for RNFL retardance versus the time to reach an endpoint for RNFL thickness. To perform this analysis, the 95% confidence limits of each parameter's measurement noise were first determined by bootstrapping from all possible pairwise differences of prelaser baseline observations within each of the 82 study eyes. In each iteration of the bootstrap, one baseline pairwise difference was sampled

Investigative Ophthalmology & Visual Science

Table 1. Study Subjects' Age, Weight, Sex, and IOP Information

						Average IOP		Peak IOP		
Animal ID	Age, y	Sex	Weight, kg	Duration, mo	No. of Laser Sessions	Control Eye	EG Eye	Control Eye	EG Eye	Cumulative IOP Difference, mm Hg-days
21676	12.5	F	5.4	10.7	9	10.5	14.8	18.0	42.7	950
22906	12.3	F	7.5	30.6	14	11.3	23.7	31.3	51.0	10,103
23499	9.9	F	4.9	12.3	7	11.0	14.7	15.3	45.7	803
23538	10.7	F	4.9	11.8	7	11.1	17.8	19.0	42.7	1,324
25357	2.6	M	5.5	17.1	8	9.0	12.0	13.3	28.7	690
25564	2.3	F	3.7	15.0	7	9.0	12.4	16.0	28.0	591
26072	1.5	F	4.1	17.2	9	8.5	10.9	15.3	32.3	458
26161	1.4	F	3.3	16.3	9	8.4	11.7	14.3	37.0	564
AM76	21.9	F	8.6	16.8	7	11.3	16.5	19.0	38.0	1,229
AM89	21.9	M	8.9	12.5	5	13.3	16.2	19.7	42.0	344
AO23	20.0	F	7.2	18.9	5	10.4	17.7	15.0	38.0	1,234
AP02	18.6	F	5.6	18.2	5	9.3	15.4	13.3	41.0	756
23506	12.5	F	4.5	6.5	2	11.2	29.0	15.0	50.7	869
23522	10.9	F	7.9	7.8	2	9.8	11.7	12.0	16.3	129
23532	11.1	F	5.0	7.1	2	11.2	19.5	16.7	38.3	549
25354	4.3	M	4.8	12.8	6	10.1	22.2	14.3	51.3	2,982
25356	4.1	M	5.1	9.9	3	8.4	20.8	13.3	44.7	2,292
25997	3.2	M	4.3	7.1	2	10.8	28.3	14.0	44.7	1,647
26163	3.2	M	4.2	11.9	6	8.9	20.3	13.7	44.0	4,819
135	10.6	M	11.4	19.1	13	10.7	14.1	18.7	40.3	1,404
137	9.6	M	13.0	14.7	2	16.4	30.5	22.3	49.0	3,725
139	9.1	F	6.2	14.7	11	12.7	21.1	19.3	52.7	3,680
140	8.8	F	6.1	11.1	5	8.9	11.1	16.0	35.7	498
15527	21.1	F	8.5	8.1	2	12.6	31.0	17.7	54.0	1,778
22100	22.6	F	5.3	41.4	6	11.2	21.6	21.0	43.0	9,916
22159	19.7	F	8.2	17.9	4	9.9	14.2	15.0	23.0	1,882
22165	21.5	F	6.0	30.4	6	11.8	24.2	22.0	52.7	9,843
24369	5.7	F	6.7	10.1	5	10.3	13.9	14.0	30.7	664
18664	15.1	F	5.9	9.2	5	8.7	10.4	12.3	15.3	251
19193	15.0	F	6.4	7.1	2	9.4	29.4	12.5	58.5	1,851
19211	14.0	F	5.9	7.3	3	10.9	13.4	19.3	27.3	291
20457	13.3	F	7.1	7.3	2	9.4	28.0	13.7	53.7	1,821
13904	15.2	F	5.7	10.6	6	13.3	19.7	20.0	55.0	1,155
28519	12.7	F	5.7	21.6	7	11.4	18.7	18.3	31.7	3,804
29435	5.9	F	5.0	18.7	8	11.4	16.0	15.0	36.3	1,747
28648	9.9	F	6.5	13.1	5	11.4	15.4	20.3	25.0	1,153
28876	7.9	F	4.9	12.2	6	14.0	21.8	20.3	49.3	1,908
28265	2.2	M	4.8	22.2	3	12.3	20.3	20.7	46.7	3,547
27806	2.1	M	4.4	22.2	5	12.3	20.5	21.7	43.0	3,394
27023	3.1	F	6.7	17.9	4	9.7	19.3	15.7	55.0	3,352
27294	3.1	F	5.4	19.0	4	9.4	18.9	15.0	48.0	3,231
Average	11.0	31 F	6.1	14.9	5.6	10.8	18.7	17.1	41.0	2,268
SD	6.6	10 M	1.9	7.4	2.9	1.7	5.8	3.8	10.7	2,488

from each of the 82 eyes and the empirical 95% confidence limits were recorded as a percentage of the mean parameter value; the final limit was taken as the average of 1000 such iterations for each RNFL parameter. Thus, the lower limit of variability from prelaser baseline values (i.e., the threshold for significant change) was defined for each eye as its prelaser baseline average minus the 95% confidence limit of measurement noise for that parameter. The endpoint for each RNFL parameter was defined as the date of the second consecutive observation below the lower limit of variability from prelaser baseline values. Thus the endpoint for each parameter represented the first sequential confirmation of significant change from baseline. McNemar's test and survival analysis were applied to compare endpoint proportions and times to endpoint, respectively. Specificities were assessed in the group of 41 fellow control (nonlasered) eyes. Figure 1 provides an example of the longitudinal course for one individual animal, including the results of the event analysis used to determine the endpoint for each parameter (Fig. 1D).

A "trend analysis" was used to compare the time to reach onset of progressive loss of RNFL retardance versus time to reach onset of progressive loss of RNFL thickness. The onset point was determined by two different methods for each longitudinal data series. The first method used segmental linear regression to determine the best fit of the following equation to the postlaser data of each EG eye:

$$\text{For } X < X_0,\ \text{RNFL value} = \text{slope}_1 \cdot X_{(\text{days from 1st laser})} + \text{intercept}_1;$$

$$\text{For } X = X_0,\ \text{RNFL value} = \text{slope}_1 \cdot X_0 + \text{intercept}_1;$$

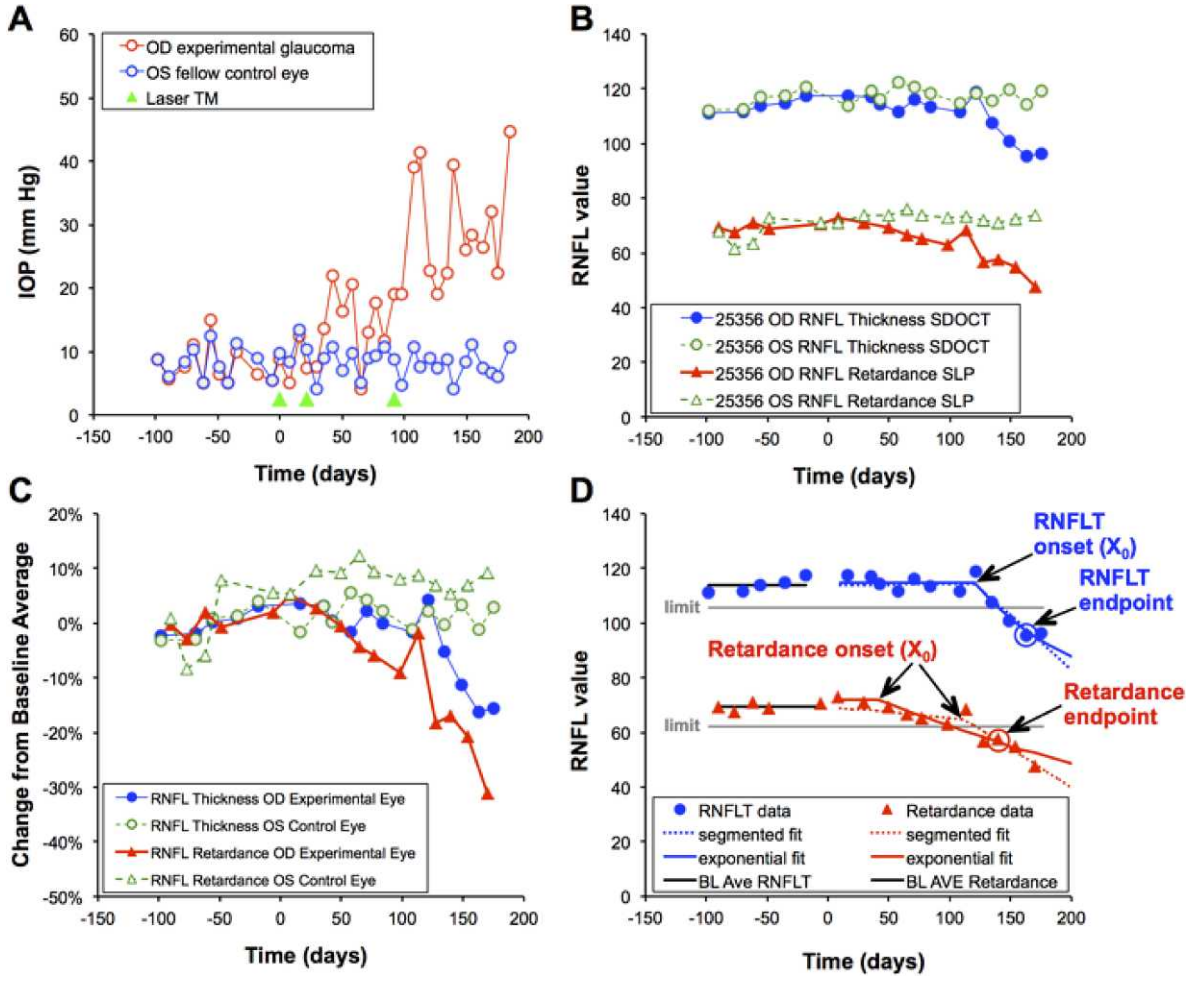

Figure 1. Example of experimental time course for a single representative animal. (**A**) IOP versus time; *green arrowheads* indicate dates of laser photocoagulation to the trabecular meshwork (TM Laser). (**B**) Peripapillary measurements of RNFL thickness (*circles*, μm) and RNFL retardance (*triangles*, nm*1.67) measured over time in the experimental eye (*filled symbols*) and control eye (*open symbols*). (**C**) RNFL data (from [**B**]) are normalized to their respective baseline averages and replotted to better compare the relative time course of each parameter, which in this case shows that RNFL retardance declined before RNFL thickness in the experimental eye. (**D**) Results of the event analysis to determine endpoint and both forms of trend analysis to determine onset of progressive loss for the experimental eye of this animal. The lower limit of measurement noise (95% confidence limit) calculated by bootstrapping for all 82 study eyes is shown by the horizontal gray line relative to the baseline average for each RNFL parameter. The second consecutive observation below this limit represents the endpoint for each parameter. This eye reached endpoint by both RNFL thickness (163 days) and RNFL retardance (140 days). The results of segmented linear regression and exponential decay fits to determine the time of onset are also shown for each parameter by the dotted and solid curves, respectively. Onset for RNFL thickness in this eye was 121 days by both segmented and exponential fits ($R^2 = 0.89$ and 0.92, respectively); onset for RNFL retardance was 113 days by segmented fit and 42 days by exponential fit ($R^2 = 0.89$ and 0.92, respectively).

$$\text{For } X > X_0,\ \text{RNFL value} = \text{slope}_2 \cdot (X - X_0) + \text{RNFL parameter value at } X_0$$

In this model, the X_0 parameter represents onset (i.e., the break point or time at which RNFL values first began to progressively decline), whereas slope_2 represents the rate of progressive decline beyond the break point. The parameter intercept_1 was constrained to equal the baseline average to determine whether the first segment of data after initiation of laser exhibited any significant trend departing from the prelaser baseline series.

The second method used nonlinear regression to determine the best fit of a model consisting of a plateau (Y_0) followed by an exponential decay described by the equation:

$$\text{For } X < X_0,\ \text{RNFL parameter value} = Y_0;$$

$$\text{For } X \geq X_0,\ \text{RNFL parameter value} = \text{Asymptote} + (Y_0 - \text{Asymptote}) \cdot \exp(-K[X - X_0])$$

In this model, the X_0 parameter again represents the onset (i.e., the time at which RNFL values first began to progressively decline) and the parameter K represents the rate of progressive decline beyond that break point.

Both models were fit to every series because it was not clear a priori which model would be most appropriate. An F-test was used to determine which was the statistically better model for each longitudinal series. However, the comparison of models returned equivocal results, so both sets of model fits are reported here, providing two separate trend analyses of the onset point comparison between RNFL retardance and thickness. Figure 1D also shows the results of the two methods of trend analysis used to determine the onset of progressive

Investigative Ophthalmology & Visual Science

loss for each parameter. Statistical comparisons of onset durations were made using Wilcoxon matched-pairs tests. All statistical analysis was performed using a commercial software package (Prism 5; GraphPad Software, Inc., La Jolla, CA).

Results

Table 1 lists the IOP results for each individual animal as well as the group averages and SD values. The average IOP values listed for each animal represent the average of all observations between the date of the first laser treatment in the EG eye and the final date prior to sacrifice; the peak values represent the peak observed within that same span. Data in Table 1 show that IOP in EG eyes was 8.0 ± 5.2 mm Hg higher, on average, than that in fellow control eyes. The peak IOP observed in EG eyes was 24.0 ± 10.3 mm Hg higher, on average, than the peak observed in the fellow control eyes. None of the EG eyes had an IOP measured above 60 mm Hg at any point during the study.

Figure 1 provides an example of the experimental course for a single individual animal (ID# 25356; see Table 1). Figure 1A shows that IOP began to increase after the second laser application to the experimental eye, which reverted until the third laser application resulted in consistent IOP elevation. Figure 1B shows the longitudinal series of peripapillary RNFL thickness and retardance measurements in both eyes, with both parameters exhibiting progressive decline toward the end of the series in the EG eye. Both parameters were normalized to their respective baseline averages and replotted in Figure 1C, which demonstrates clearly that RNFL retardance declined before RNFL thickness in this EG eye. Figure 1D shows the results of the event analysis used to determine endpoint. This eye reached endpoint by both RNFL retardance (140 days) and RNFL thickness (163 days), thus 3 weeks earlier by RNFL retardance. As will be shown in the subsequent section, this gap was slightly less than the average observed for the whole study group.

Results of Event Analysis for Endpoint Comparison

Of the 41 EG eyes in this study, 29 (71%) of the EG eyes reached endpoint by RNFL retardance and 25 (61%) reached endpoint by RNFL thickness. In total, 33 (80%) reached endpoint by at least one of the RNFL parameters and 21 (51%) reached endpoint by both RNFL parameters. Eight EG eyes (20%) did not reach endpoint by either RNFL measure before being sacrificed for other histopathologic studies. Of the 33 EG eyes reaching any endpoint, a larger proportion reached endpoint first by RNFL retardance ($n = 26$, 79%) than did by RNFL thickness ($n = 7$, 21%; $\chi^2 = 9.8$, two-tailed, $P = 0.002$, McNemar's test). The odds ratio was thus 3.7, with a 95% confidence interval ranging from 1.6 to 10.1 times more likely to reach endpoint first by RNFL retardance than by RNFL thickness.

Among the 33 EG eyes reaching any endpoint (i.e., by either RNFL measure), the median duration to endpoint (from first laser) was 135 days for RNFL retardance and 240 days for RNFL thickness ($P = 0.002$, Wilcoxon test), a lead time of 105 days for RNFL retardance. The average duration to endpoint in this group was 198 days for RNFL retardance and 263 days for RNFL thickness, thus 65 days earlier for RNFL retardance. In this analysis, if an eye did not reach endpoint, its duration was assigned to be the interval between the first laser and the final observation; thus, it is possible that the lead time for RNFL retardance endpoint would have been even greater. To examine this further, the same comparison was performed on the subgroup of 21 EG eyes that reached endpoint by both RNFL parameters. In this group, the median duration to endpoint was 120 days for RNFL retardance and 223 days for RNFL thickness ($P = 0.003$, Wilcoxon test), a lead time of 103 days for RNFL retardance, essentially identical to that of the larger group. The average durations in this subgroup were 161 days for RNFL retardance and 202 days for RNFL thickness, 41 days earlier for RNFL retardance. Not surprisingly, the durations to reach endpoint were slightly faster in the subgroup of 21 EG eyes that reached endpoint by *both* RNFL parameters, since reaching both endpoints is more likely to occur in the more rapidly progressing eyes. The results of the survival analysis (Fig. 2) also indicated a shorter time to reach endpoint by RNFL retardance than by RNFL thickness ($\chi^2 = 11.7$, $P = 0.0006$, log-rank Mantel-Cox test and $\chi^2 = 12.0$, $P = 0.0005$, Gehan-Breslow-Wilcoxon test).

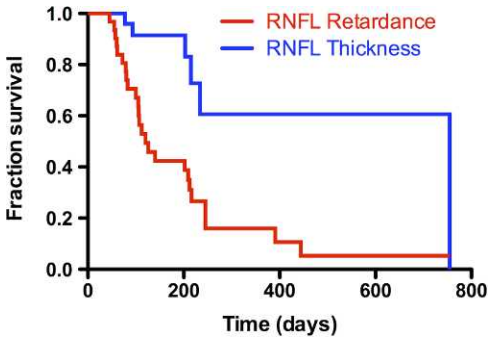

Figure 2. Survival curves comparing endpoints reached first by peripapillary RNFL retardance with endpoints reached first by RNFL thickness (total of $n = 41$ EG eyes; each was censored at the first endpoint reached, or at date of sacrifice if no endpoint was reached).

The event analysis used to determine endpoint was based on each parameter's inherent measurement noise. The parameter with the relatively wider measurement noise limits should be at a disadvantage in this analysis if both parameters were otherwise measuring the same underlying anatomic feature. However, measurement noise was approximately 50% larger for RNFL retardance than that for RNFL thickness (10.33% vs. 6.96%), which suggests that the greater likelihood of reaching endpoint earlier by RNFL retardance occurs despite its relatively greater variability (i.e., more "distant" endpoint threshold for achieving significant change below baseline). Consistent with its larger variability measured during baseline, the specificity derived from the group of 41 fellow control eyes was lower for RNFL retardance (90%) than that for RNFL thickness (100%); that is, four control eyes met the endpoint definition for RNFL retardance, whereas none did so for RNFL thickness. Increasing the criterion for endpoint to two sequential confirmations increased specificity of RNFL retardance to 98%, but also substantially reduced the number of endpoints among EG eyes for both parameters, since several animals were sacrificed without a subsequent imaging session. The example shown in Figure 1D shows an animal that would have just met this stricter criterion prior to sacrifice, whereas others did not.

If RNFL retardance endpoints occur earlier than RNFL thickness endpoints during the course of progressive damage, then the relative degree of damage measured at the other parameter's endpoint should reflect this difference. That is, the relative degree of damage measured by RNFL thickness at the retardance endpoint should be relatively small, whereas the degree of damage measured by retardance at the RNFL thickness endpoint should be worse. The results were consistent with this prediction. At RNFL thickness endpoint ($n = 25$ EG eyes), RNFL retardance was reduced by 21.1 ±

Investigative Ophthalmology & Visual Science

Table 2. Results of Trend Analysis for Comparing Duration to Onset of Progressive RNFL Retardance Loss With Duration to Onset of RNFL Thickness Loss

***n* = 33 Endpoint by Either RNFL Parameter**	**RNFL Retardance**	**RNFL Thickness**	**Difference**	**Wilcoxon *P* Value**
X_0 (segmented)	115 d	170 d	55 d	0.002
R^2 (segmented)	0.78	0.81		0.24
X_0 (exponential)	43 d	121 d	78 d	0.001
R^2 (exponential)	0.85	0.83		0.48
***n* = 21 Endpoint by Both RNFL Parameters**				
X_0 (segmented)	114 d	145 d	31 d	0.008
R^2 (segmented)	0.89	0.89		0.30
X_0 (exponential)	42 d	148 d	102 d	0.01
R^2 (exponential)	0.91	0.87		0.33

The table lists the median values for the X_0 parameter derived from the segmented linear model and the exponential decay model as well as a goodness-of-fit metric (median R^2) in each case.

13.0% (range: 8% above baseline to 44% below). In contrast, at RNFL retardance endpoint ($n = 29$ EG eyes), RNFL thickness was reduced by only 5.9 ± 8.3% (range: 9% above baseline to 27% below, $P < 0.0001$).

Results of Trend Analysis for Onset Comparison

Figure 1D shows both forms of trend analysis used to determine the onset of progressive loss for each parameter. In this EG eye, the onset of progressive loss of RNFL thickness was determined to be 121 days by both the segmental linear fit and the exponential fit ($R^2 = 0.89$ and 0.92, respectively), whereas the onset for RNFL retardance was 113 days by the segmented fit ($R^2 = 0.89$) and 42 days by the exponential fit ($R^2 = 0.92$). Each model has potential advantages, for example, if progressive loss stabilizes, such as in the case of reaching a "floor," the exponential decay model should provide the better fit to the series. In contrast, if the period between the first laser and the onset point contains any systematic trend, then the segmented fit should provide a better fit than the plateau with exponential decay. The results of formal comparison for each series (by *F*-test) indicate that approximately half of the cases are described better by the segmental linear fit than by the exponential model: 23 of the 41 series for RNFL thickness and 20 of the 41 series for RNFL retardance were better fit by the segmented model. Thus, rather than risk any potential bias due to choice of model, the results are presented for both models in the next section and Table 2.

For the group of 33 EG eyes that reached an endpoint by at least one RNFL parameter, the median time (from first laser) to onset determined by the segmental linear fit was 115 days for RNFL retardance and 170 days for RNFL thickness ($P = 0.002$, Wilcoxon test), a lead of 55 days for RNFL retardance (Table 2). There was no difference in the goodness-of-fit for the segmented linear model between RNFL retardance and RNFL thickness ($P = 0.24$, Table 2). Using the exponential model to determine onset resulted in a similar lead time of 78 days for RNFL retardance ($P = 0.001$, Table 2). When the comparisons were limited to just the subgroup of 21 EG eyes that reached endpoint by *both* RNFL parameters, the median time to onset determined by the segmented was 114 days for RNFL retardance and 145 days for RNFL thickness ($P = 0.008$, Table 2), representing a lead time of 31 days for RNFL retardance. The results of fitting the exponential model in this subgroup of 21 EG eyes also returned a lead time of 102 days for RNFL retardance ($P = 0.01$, Table 2). Model fits were generally better for these 21 eyes with worse progression (i.e., those reaching an endpoint by both RNFL parameters).

Using the results of the exponental decay model to compare Y_0 (the value of the plateau) with the prelaser baseline average revealed a small but significant increase of RNFL thickness during the period between the first laser and the onset of progressive decline (median of 2.4%, $P < 0.0001$, Wilcoxon). In contrast, Y_0 for RNFL retardance was closer to its prelaser baseline average values (median difference of 0.4% above baseline, $P = 0.09$).

A comparison of parameters from the segmented linear model other than the break point (X_0) revealed the following results: first, the slope of the initial segment from the segmented linear model was not significantly different from zero for either RNFL thickness (median slope: 0.4% per month increase, $P = 0.05$) or RNFL retardance (median slope: 0.6% per month decrease, $P > 0.32$). Second, there was no difference between RNFL retardance and RNFL thickness in terms of the rate of progression beyond the onset point, as measured by the slope of the second segment ($P = 0.37$). The median rate of loss for RNFL retardance and RNFL thickness, respectively, was 7.2% per month, 6.5% per month of the baseline average value in each eye. The rate of RNFL thickness loss was unrelated to mean IOP (Spearman $R = -0.22$, $P = 0.23$) and only modestly correlated with peak IOP ($R = -0.39$, $P = 0.03$), whereas the rate of retardance loss was not correlated with either IOP parameter (mean IOP: $R = -0.04$, $P = 0.83$; peak IOP: $R = -0.10$, $P = 0.58$). RNFL damage at the final available time point (relative to baseline) was better correlated with peak IOP than mean IOP for both RNFL thickness (mean IOP: $R = -0.35$, $P = 0.02$; peak IOP: $R = -0.56$, $P = 0.0001$) and retardance (mean IOP: $R = -0.02$, $P = 0.88$; peak IOP: $R = -0.26$, $P = 0.10$). This is consistent with previous observations based on shorter analysis windows[22] and suggests some individual eyes are more or less susceptible (or resilient) than other eyes to a given level of IOP elevation.

Discussion

By following the longitudinal course of RNFL damage in this study through further stages of damage, we found that the onset of progressive loss of RNFL retardance measured by SLP

occurs earlier than the onset of RNFL thinning measured by SD-OCT in a nonhuman primate model of experimental glaucoma. This is consistent with the findings of our previous study, which was based on a different analysis limited to earlier stages of RNFL damage (around the onset of ONH surface topography change).[8] In the current study, we also found that endpoint events are reached more frequently and earlier by SLP measures of RNFL retardance than by SD-OCT measures of RNFL thickness. Since it is thought that normal RNFL birefringence is due to the highly ordered structural array of axonal cytoskeletal proteins,[10–13] these results add further evidence to support the hypothesis that axonal cytoskeletal disruption precedes axon loss within the glaucomatous RNFL. Histopathologic evaluation of the RNFL is under way in half of the animals whose in vivo data are reported here.

Another recent longitudinal study of experimental glaucoma in nonhuman primates found that RNFL reflectivity, but not phase retardance or birefringence, decreased over time.[23] However, this study was based on only three subjects, only one of which developed measurable thinning of the RNFL over the duration of follow-up. Moreover, RNFL reflectance also decreased in the three fellow control eyes (albeit at approximately half the rate of the average decline observed in the glaucomatous eyes). The elegant device custom-built for that study to measure all four RNFL parameters simultaneously used a 1060-nm center wavelength swept source, which has 3-fold lower axial resolution and 2- to 2.5-fold lower transverse resolution than the SD-OCT device used in our study. Their study also used spatial averaging to reduce speckle noise (in contrast to temporal averaging used in ours), which would have further reduced spatial resolution; thus, the capabilities for visualization and segmentation of RNFL boundaries (particularly the posterior boundary; see, e.g., Fig. 3 in the study reported by Dwelle et al.[23]) will have been relatively limited, which is also critical to the calculations of RNFL phase retardance and birefringence. This might be one reason why repeatability of all four parameters was relatively poor in that study, limiting detection of specific changes.[23] Nevertheless, other studies in both clinical[24,25] and laboratory[26] settings have also observed altered reflectance of the glaucomatous RNFL, suggesting that this phenomenon might be another sensitive indicator of early axonal damage, which is also likely to reflect cytoskeletal abnormalities.[27]

It is also important to note that a recent prospective, longitudinal clinical study found that progression occurred more frequently and earlier for SD-OCT measurements of RNFL thickness as compared with polarimetric measurments of RNFL retardance.[28] This contrasts with the findings of our study and the hypothesis that axonal cytoskeletal disruption precedes thinning in the glaucomatous RNFL. One possibility for the discrepancy is that the glaucoma patients followed by Xu and colleagues[28] may have already had substantial RNFL damage at study baseline, leaving little dynamic range for detection of further retardance changes. Additional clinical studies, perhaps focused on early-stage glaucoma, might help explain some of the discrepancy; meanwhile, the results reported by Xu et al.[28] raise questions about the generalizability of our current findings to clinical management of glaucoma patients.

In addition to the limitations discussed in our previous report about the experimental model and study design,[8] there are additional limitations specific to this study. First, we used a single sequential confirmation as the criterion defining the endpoint of progressive change from baseline in the event analysis. Specificity assessed in the group of 41 fellow control eyes was higher for RNFL thickness (100%) than it was for RNFL retardance (90%), reflecting in part the slightly greater variability found for retardance measured by SLP over RNFL thickness measured by SD-OCT (measurement noise was 10% vs. 7%, respectively). Alternative criteria were also analyzed and rejected for the following reasons. An endpoint criterion defined by a single point resulted in a larger number of EG eyes reaching an endpoint (38 rather than 33), but also in an unacceptably low specificity for both RNFL parameters (<90%). Endpoint criteria defined by two confirmations resulted in higher specificity (98% for retardance and 100% for RNFL thickness), but eight fewer animals reached an endpoint by that definition prior to sacrifice (25 rather than 33). Thus, we chose an endpoint definition that would maximize the proportion of EG eyes reaching an RNFL endpoint while maintaining adequately high specificity. The results were otherwise similar in that the time to reach endpoint was still 97 days shorter for retardance ($P = 0.02$) as compared with RNFL thickness using the stricter endpoint definition.

In our previous report[8] we discussed the potential impact of differing dynamic ranges between RNFL retardance and RNFL thickness (i.e., the "floor" effect documented for RNFL thickness[29,30] might be lower or even absent for RNFL retardance; the latter is not yet known with precision). However, the results of the analyses performed in this study should be robust to potential differences in dynamic range because the onset point derived by fitting either the segmented linear model or the exponential model would not be altered by alternative scaling of the ordinal values. Similarly, the endpoint definition would not be altered by alternative scaling. Thus, the possibility that the dynamic range of RNFL thickness is compressed relative to that for RNFL retardance should not affect the conclusions of this study. However, the results of this study—based on a different analysis and larger sample size—confirm the observation from our previous study[8] that there is a small increase of RNFL thickness prior to the onset of progressive decline. The anatomic and physiologic basis for this increase is not yet apparent, but it might account for some of the "lead time" found for progressive decline of RNFL retardance.

This study was also limited to the overall average values of peripapillary RNFL retardance and thickness. Previous studies have shown that birefringence is not uniform around the optic nerve head; RNFL axon bundles at the superior and inferior poles exhibit greater retardance per unit thickness than do the bundles of the temporal and nasal sectors.[14,31–33] This means that relatively isolated loss of axons at one of the vertical poles could exert greater influence on the overall average value of peripapillary RNFL retardance. However, this nonhuman primate model of experimental glaucoma tends to result in diffuse RNFL damage such that the time course of relative loss (e.g., when normalized to baseline average) is similar for the overall peripapillary average and any given sector. Moreover, when analyzed separately by quadrants, the lead time still exists for RNFL retardance versus thickness (not shown). Formal analysis of radial sectors and varying eccentricity from the optic nerve head are under way now that we have developed the methods and software to effectively colocalize the SLP and SD-OCT data sets (see, e.g., Reynaud J, et al. *IOVS* 2013;54:ARVO E-Abstract 4844 and Huang et al.[31]).

In summary, this study demonstrates that the onset of progressive loss of RNFL retardance measured by SLP occurs earlier than the onset of RNFL thinning measured by SD-OCT. Endpoints of progressive loss from baseline also occurred more frequently and earlier for RNFL retardance as compared with RNFL thickness. It is likely that these results reflect a stage of glaucomatous axonopathy, whereby axonal cytoskeletal disruption is present prior to thinning of axonal caliber. This might also represent a reversible stage of injury response. Future studies are planned to investigate this possibility.

Investigative Ophthalmology & Visual Science

Acknowledgments

The authors thank Galen Williams, Christy Hardin, and Luke Reyes for their expert technical assistance during data collection.

Supported by National Eye Institute/National Institutes of Health Grants R01-EY019327 (BF), R01-EY011610 (CFB), and R01-EY019939 (LW); Glaucoma Research Foundation (BF); American Health Assistance Foundation (BF); Legacy Good Samaritan Foundation; Heidelberg Engineering, GmbH, Heidelberg, Germany (equipment and unrestricted research support); Carl Zeiss Meditec, Inc. (equipment).

Disclosure: **B. Fortune**, Carl Zeiss Meditec, Inc. (F), Heidelberg Engineering, GmbH (F); **C.F. Burgoyne**, Heidelberg Engineering, GmbH (F, C); **G. Cull**, None; **J. Reynaud**, None; **L. Wang**, None

References

1. Hoyt WF, Newman NM. The earliest observable defect in glaucoma? *Lancet*. 1972;1:692–693.
2. Hoyt WF, Frisen L, Newman NM. Fundoscopy of nerve fiber layer defects in glaucoma. *Invest Ophthalmol*. 1973;12:814–829.
3. Sommer A, Katz J, Quigley HA, et al. Clinically detectable nerve fiber atrophy precedes the onset of glaucomatous field loss. *Arch Ophthalmol*. 1991;109:77–83.
4. Zangwill LM, Bowd C. Retinal nerve fiber layer analysis in the diagnosis of glaucoma. *Curr Opin Ophthalmol*. 2006;17:120–131.
5. Townsend KA, Wollstein G, Schuman JS. Imaging of the retinal nerve fibre layer for glaucoma. *Br J Ophthalmol*. 2009;93:139–143.
6. Cull GA, Reynaud J, Wang L, Cioffi GA, Burgoyne CF, Fortune B. Relationship between orbital optic nerve axon counts and retinal nerve fiber layer thickness measured by spectral domain optical coherence tomography. *Invest Ophthalmol Vis Sci*. 2012;53:7766–7773.
7. Strouthidis NG, Fortune B, Yang H, Sigal IA, Burgoyne CF. Longitudinal change detected by spectral domain optical coherence tomography in the optic nerve head and peripapillary retina in experimental glaucoma. *Invest Ophthalmol Vis Sci*. 2011;52:1206–1219.
8. Fortune B, Burgoyne CF, Cull GA, Reynaud J, Wang L. Structural and functional abnormalities of retinal ganglion cells measured in vivo at the onset of optic nerve head surface change in experimental glaucoma. *Invest Ophthalmol Vis Sci*. 2012;53:3939–3950.
9. Weinreb RN, Dreher AW, Coleman A, Quigley H, Shaw B, Reiter K. Histopathologic validation of Fourier-ellipsometry measurements of retinal nerve fiber layer thickness. *Arch Ophthalmol*. 1990;108:557–560.
10. Zhou Q, Knighton RW. Light scattering and form birefringence of parallel cylindrical arrays that represent cellular organelles of the retinal nerve fiber layer. *Applied Optics*. 1997;36:2273–2285.
11. Huang XR, Knighton RW. Linear birefringence of the retinal nerve fiber layer measured in vitro with a multispectral imaging micropolarimeter. *J Biomed Opt*. 2002;7:199–204.
12. Huang XR, Knighton RW. Microtubules contribute to the birefringence of the retinal nerve fiber layer. *Invest Ophthalmol Vis Sci*. 2005;46:4588–4593.
13. Fortune B, Wang L, Cull G, Cioffi GA. Intravitreal colchicine causes decreased RNFL birefringence without altering RNFL thickness. *Invest Ophthalmol Vis Sci*. 2008;49:255–261.
14. Pocock GM, Aranibar RG, Kemp NJ, Specht CS, Markey MK, Rylander HG III. The relationship between retinal ganglion cell axon constituents and retinal nerve fiber layer birefringence in the primate. *Invest Ophthalmol Vis Sci*. 2009;50:5238–5246.
15. Fortune B, Cull GA, Burgoyne CF. Relative course of retinal nerve fiber layer birefringence and thickness and retinal function changes after optic nerve transection. *Invest Ophthalmol Vis Sci*. 2008;49:4444–4452.
16. Fortune B, Yang H, Strouthidis NG, et al. The effect of acute intraocular pressure elevation on peripapillary retinal thickness, retinal nerve fiber layer thickness, and retardance. *Invest Ophthalmol Vis Sci*. 2009;50:4719–4726.
17. Weinreb RN, Bowd C, Zangwill LM. Scanning laser polarimetry in monkey eyes using variable corneal polarization compensation. *J Glaucoma*. 2002;11:378–384.
18. Choplin NT, Zhou Q, Knighton RW. Effect of individualized compensation for anterior segment birefringence on retinal nerve fiber layer assessments as determined by scanning laser polarimetry. *Ophthalmology*. 2003;110:719–725.
19. GDxVCC Instrument Manual. *RNFL Analysis with GDxVCC: A Primer and Clinical Guide*. San Diego, CA: Laser Diagnostic Technologies, Inc.; 2004.
20. Gaasterland D, Kupfer C. Experimental glaucoma in the rhesus monkey. *Invest Ophthalmol*. 1974;13:455–457.
21. Quigley HA, Hohman RM. Laser energy levels for trabecular meshwork damage in the primate eye. *Invest Ophthalmol Vis Sci*. 1983;24:1305–1307.
22. Gardiner SK, Fortune B, Wang L, Downs JC, Burgoyne CF. Intraocular pressure magnitude and variability as predictors of rates of structural change in non-human primate experimental glaucoma. *Exp Eye Res*. 2012;103:1–8.
23. Dwelle J, Liu S, Wang B, et al. Thickness, phase retardation, birefringence, and reflectance of the retinal nerve fiber layer in normal and glaucomatous non-human primates. *Invest Ophthalmol Vis Sci*. 2012;53:4380–4395.
24. van der Schoot J, Vermeer KA, de Boer JF, Lemij HG. The effect of glaucoma on the optical attenuation coefficient of the retinal nerve fiber layer in spectral domain optical coherence tomography images. *Invest Ophthalmol Vis Sci*. 2012;53:2424–2430.
25. Vermeer KA, van der Schoot J, Lemij HG, de Boer JF. RPE-normalized RNFL attenuation coefficient maps derived from volumetric OCT imaging for glaucoma assessment. *Invest Ophthalmol Vis Sci*. 2012;53:6102–6108.
26. Huang XR, Zhou Y, Kong W, Knighton RW. Reflectance decreases before thickness changes in the retinal nerve fiber layer in glaucomatous retinas. *Invest Ophthalmol Vis Sci*. 2011;52:6737–6742.
27. Huang XR, Knighton RW, Cavuoto LN. Microtubule contribution to the reflectance of the retinal nerve fiber layer. *Invest Ophthalmol Vis Sci*. 2006;47:5363–5367.
28. Xu G, Weinreb RN, Leung CK. Retinal nerve fiber layer progression in glaucoma: a comparison between retinal nerve fiber layer thickness and retardance. *Ophthalmology*. In press.
29. Sihota R, Sony P, Gupta V, Dada T, Singh R. Diagnostic capability of optical coherence tomography in evaluating the degree of glaucomatous retinal nerve fiber damage. *Invest Ophthalmol Vis Sci*. 2006;47:2006–2010.
30. Chan CK, Miller NR. Peripapillary nerve fiber layer thickness measured by optical coherence tomography in patients with no light perception from long-standing nonglaucomatous optic neuropathies. *J Neuroophthalmol*. 2007;27:176–179.
31. Huang XR, Bagga H, Greenfield DS, Knighton RW. Variation of peripapillary retinal nerve fiber layer birefringence in normal human subjects. *Invest Ophthalmol Vis Sci*. 2004;45:3073–3080.
32. Cense B, Chen TC, Park BH, Pierce MC, de Boer JF. Thickness and birefringence of healthy retinal nerve fiber layer tissue measured with polarization-sensitive optical coherence tomography. *Invest Ophthalmol Vis Sci*. 2004;45:2606–2612.
33. Rylander HG III, Kemp NJ, Park J, Zaatari HN, Milner TE. Birefringence of the primate retinal nerve fiber layer. *Exp Eye Res*. 2005;81:81–89.

Investigative Ophthalmology & Visual Science